# Ground and Excited States of the Monomer and Dimer of Certain Carboxylic Acids

**U. Lourderaj, Kousik Giri, and N. Sathyamurthy***

*Department of Chemistry, Indian Institute of Technology Kanpur, Kanpur 208 016 India*

*Received: November 9, 2005; In Final Form: December 29, 2005*

The ground-state properties of the monomer and the dimer of formic acid, acetic acid, and benzoic acid have been investigated using Hartree−Fock (HF) and density functional theory (DFT) methods using the 6-311++G-(d,p) basis set. Some of the low-lying excited states have been studied using the time-dependent density functional theory (TDDFT) with LDA and B3LYP functionals and also employing complete-active-space-self-consistent-field (CASSCF) and multireference configuration interaction (MRCI) methodologies. DFT calculations predict the ground-state geometries in quantitative agreement with the available experimental results. The computed binding energies for the three carboxylic acid dimers are also in accord with the known thermodynamic data. The TDDFT predicted wavelengths corresponding to the lowest energy n−$\pi$* transition in formic acid (214 nm) and acetic acid (214 nm) and the $\pi-\pi$* transition in benzoic acid (255 nm) are comparable to the experimentally observed absorption maxima. In addition, TDDFT calculations predict qualitatively correctly the blue shift (4−5 nm) in the excitation energy for the $\pi-\pi$* transition in going from the monomer to the dimer of formic acid and acetic acid and the red shift (∼19 nm) in $\pi-\pi$* transition in going from benzoic acid monomer to dimer. This also indicates that the electronic interaction arising from the hydrogen bonds between the monomers is marginal in all three carboxylic acids investigated.

## 1. Introduction

Carboxylic acids (RCOOH) play an important role in many processes in chemistry and biology. Their monomers can exist in two forms: cis (syn) and trans (anti), as illustrated in Figure 1. The former has the carboxylic hydrogen atom pointing toward the R group, while the latter has the two pointing away from each other. A 180° rotation about the C−O single bond would transform one isomer into the other. Their acidity is decided by electronic and conformational factors. They form cyclic dimers, with two hydrogen bonds acting as a bridge between the monomers. The cyclic dimer thus formed can undergo double proton transfer and has been a subject of interest for many decades, partly because they can serve as prototypes for DNA base pairs.

The literature available on the structure and spectral properties of carboxylic acids is substantial. Although formic acid (FA) can be considered as a prototype aliphatic acid, it differs from acetic acid (AA) in that the presence of the methyl group in the latter alters the properties of the molecule to a noticeable extent. Therefore, both of them deserve to be studied individually. Benzoic acid (BA) is the first member of the aromatic carboxylic acids. Hence a systematic study of the ground and excited states of all three acids was undertaken.

The rotational spectra of the trans and cis isomers of formic acid have been well-recorded, and the structures of both isomers are well-known.[1−6] The trans isomer of formic acid was found to be more stable than the cis one by 3.86 kcal/mol,[2] and the barrier for rotation was estimated to be 13.8 kcal/mol.[7] The vibrational spectra have been recorded, and most of the frequencies have been assigned.[8,9] The first excited state ($S_1$) of formic acid (arising from the n−$\pi$* transition) was investigated as early as 1943, when Sugarman[10] reported a structured

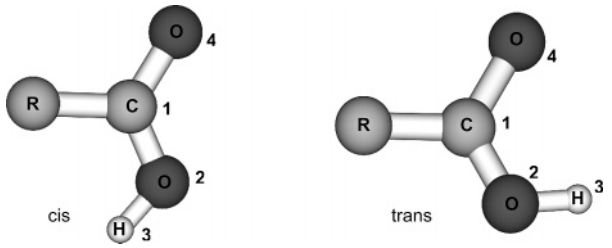


**Figure 1.** Cis (syn) and trans (anti) forms of carboxylic acid monomers: R = H, formic acid; R = $CH_3$, acetic acid; R = $C_6H_5$, benzoic acid.

electronic spectrum in the range of 226−260 nm. Barnes and Simpson[11] extended it to the vacuum ultraviolet (125−185 nm) region. Ng and Bell[12] reported additional sharp bands in the near-UV (225−250 nm) region. Their studies suggested that formic acid is nonplanar in the excited state. Singleton et al.[13] found the absorption cross-section to be a maximum at 215 nm. A laser-induced fluorescence (LIF) investigation identified the band origin (267 nm) and resolved the vibrational structures.[14] The LIF excitation spectra recorded subsequently by Beaty-Travis et al.[15] gave an insight into the structural conformers arising from torsion and wagging modes in the first excited state. Nagakura et al.[16] recorded the absorption cross-section in the vacuum-UV region and identified the peak at 159 nm with the $\pi-\pi$* transition.

Formic acid dimer (FAD) exists as a ring structure (see Figure 2) in which the two monomer units are linked by hydrogen bonds that add to its stability. The dimerization energy of FAD was reported to be 14.8 kcal/mol by Clague and Bernstein.[17] Because of the symmetry of the ring structure, FAD has no dipole moment and hence it is not possible to record its rotational spectrum. Matylitsky et al.[18] determined the cyclic structure of FAD using a time-resolved structure selective spectroscopy.

* To whom correspondence should be addressed. E-mail: nsath@iitk.ac.in.

10.1021/jp056491x CCC: $33.50 
Published on Web 02/04/2006

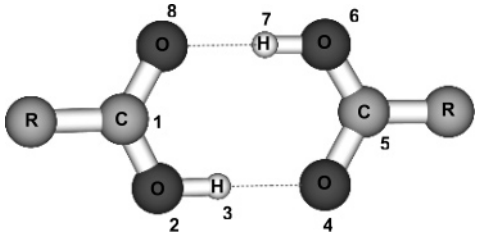


**Figure 2.** Structure of the carboxylic acid dimers: R = H, formic acid; R = $CH_3$, acetic acid; R = $C_6H_5$, benzoic acid.

Using matrix isolation under supersonic jet conditions, Halupka and Sander[19] were able to record the infrared spectrum of the dimer and assign a number of frequencies. Jet-cooled infrared spectra of FAD and its isotopomers have been reported by Ito and Nakanaga.[20] Georges et al.[21] recorded the Fourier transform infrared spectra of the dimer under jet-cooled and room-temperature conditions. Madeja and Havenith[22] have measured the tunneling splitting for $(DCOOH)_2$, and this has been assigned to the zero-point level by Smedarchina et al.[23,24]

Studies on the excited states of FAD have been limited. As mentioned earlier, Barnes and Simpson[11] recorded the absorption spectrum of FAD in the vacuum-ultraviolet region in 1963. Singleton et al.[13] reported an absorption maximum for the dimer at 205 nm. Carnovale et al.[25] measured the photoelectron spectrum of FAD in the gas phase and suggested that the $\sigma$ molecular orbitals (MO) of the monomers interacted much more than the $\pi$ orbitals. To the best of our knowledge, there has not been any other study on the excited states of FAD.

The geometrical parameters of acetic acid monomer as well as the dimer (AAD) in the ground electronic state are well-established.[26,27] The anti conformer is known to be more stable than the syn by 6.5 kcal/mol,[28] and the dimer exists in a cyclic form with hydrogen bonds linking the two anti conformers. Ovaska[29] undertook an infrared spectral study of the normal and deuterated acetic acid dimers. Halupka and Sander[19] have examined the infrared spectrum of AA and AAD under matrix isolation condition. Supersonic jet spectra for both AA and AAD have been reported recently by Häber et al.[30] Vacuum-UV absorption studies of acetic acid by Barnes and Simpson[11] revealed a spectrum that was much less structured than that of FA and that the spectrum for the dimer was blue-shifted when compared to that of the monomer of acetic acid. Nagakura et al.[16] reported a peak at 160 nm for AA that was blue-shifted by 1 nm from the absorption peak of FA. Orlando and Tyndall[31] recorded the gas-phase UV absorption spectrum for acetic acid monomer and observed a broad maximum around 207 nm. They also recorded the absorption spectrum for the dimer and found the peak intensity for the dimer to be about double that of the monomer. They showed that the absorption cross-section increased monotonically with energy, with the maximum occurring at a wavelength short of 205 nm. Recently, Hintze et al.[32] have reported the absorption cross-sections for both the monomer and the dimer of acetic acid. The monomer shows maximum absorption at 209 nm and the dimer at 203 nm. They confirm that the peak intensity for AAD is indeed double that of AA.

The experimental geometrical parameters for benzoic acid were reported by Bruno and Randaccio[33] in 1980. The heat of formation of the cyclic dimer was estimated to be 16 kcal/mol.[34,35] Proton tunneling in the dimer (BAD) has been investigated in the ground electronic state, and a tunneling splitting of 1107 MHz was observed.[36] This has been assigned recently to the zero-point level by Smedarchina et al.[24] Recently, IR studies have been carried out using fluorescence-dip and jet-cooled techniques both in the ground and the first excited state, for the monomer as well as the dimer of benzoic acid.[37,38] Ito et al.[39] reported a slight red shift in absorption maximum on dimerization. The absorption spectrum of benzoic acid shows three bands, labeled as C, B, and A, near 280, 230, and 190 nm, respectively.[40] Baum and McClure[41] reported the band origin at 285 nm for the excited singlet and 364 nm for the triplet of the dimer in benzene single crystal. Meijer et al.[42] have investigated the gas-phase $S_1 \leftarrow S_0$ absorption spectrum of BA monomer (origin, 278 nm) and the dimer (origin, 280 nm) by laser jet-cooled spectroscopy. There have been extensive studies of the dimer in the excited state by Poeltl and McVey[43,44] using free-jet expansion technique. Using an LIF study, Nandi and Chakraborty[45] have reported on the hydrogen bond induced vibronic mixing in benzoic acid dimer (band origin, 280 nm).

Theory has kept pace with experiment when it comes to the properties of the ground state of these acids. A variety of theoretical methods have been used to predict the ground-state geometry of all three acids mentioned above. In addition, it has been confirmed that the trans (anti) form is more stable than the cis (syn) and that the carboxylic acid dimer is indeed cyclic with a binding energy that is comparable to what has been determined from experiments. Alternative geometries possible for the dimer have also been examined at various levels of theory.[46,47] Several papers have focused on the changes in the monomer geometry on dimer formation, resonance-assisted hydrogen bonding, infrared and Raman spectra,[48] and double proton transfer in the dimer. For a recent review of the literature on formic acid and acetic acid, the reader is referred to ref 49.

Quantitative prediction of the properties of the excited electronic states requires calculations that include electron correlation. This was demonstrated early on by Peyerimhoff and Buenker[50] and Demoulin[51] for formic acid. However, ab initio calculations on the excited-state properties of all three acids have remained limited in scope until this date. Therefore, we have undertaken a detailed study of carboxylic acid monomers and dimers, $(RCOOH)_2$, where R = H, $CH_3$, and $C_6H_5$ in their ground and excited states using a variety of theoretical methods described below.

## 2. Methodology

The ground-state properties of the monomer and the dimer of formic acid, acetic acid, and benzoic acid have been investigated using Hartree−Fock (HF) and density functional theoretic (DFT) methods[52] using the 6-311++G(d,p) basis set. The excited states have been studied using the time-dependent density functional theoretic (TDDFT) method[53,54] using LDA[52] and B3LYP[55,56] functionals and also employing complete-active-space-self-consistent-field (CASSCF)[57,58] and multireference configuration interaction (MRCI)[59,60] methodologies. The choice of active space is known to be critical in CASSCF and MRCI calculations. However, only a maximum of eight active orbitals with eight active electrons was used because of the limitation in the available resources. The nature of excitation was assigned on the basis of the major contribution. All the HF and DFT calculations were carried out using the GAUSSIAN 98 [61] suite of programs. For the CASSCF and MRCI calculations, the MOLPRO 2000.1 [62] package was used.

## 3. Results and Discussion

**3.1. Formic Acid Monomer.** The ground-state geometry of the trans form of formic acid monomer was optimized at HF and DFT(LDA, B3LYP) levels of theory using 6-311++G(d,p) basis set. The resulting geometric parameters are listed in Table

**TABLE 1: Ground-State Geometric Parameters for *trans*-Formic Acid, -Acetic Acid, and -Benzoic Acid**

| | FA | | | AA | | | BA | | |
|---|---|---|---|---|---|---|---|---|---|
| param | HF[a] | DFT/B3LYP[a] | expt[b] | HF[a] | DFT/B3LYP[a] | expt[c] | HF[a] | DFT/B3LYP[a] | expt[d] |
| $r_{12}$(C−O)/Å | 1.321 | 1.346 | 1.343 | 1.331 | 1.358 | 1.364(0.003) | 1.329 | 1.359 | 1.29 |
| $r_{23}$(O−H)/Å | 0.947 | 0.971 | 0.972 | 0.946 | 0.969 | 0.97 | 0.946 | 0.968 | |
| $r_{14}$(C═O)/Å | 1.177 | 1.199 | 1.202 | 1.182 | 1.205 | 1.214(0.003) | 1.185 | 1.209 | 1.24 |
| $\theta_{123}$/deg | 109.4 | 107.9 | 106.3 | 108.8 | 107.1 | 107.0 | 108.3 | 106.6 | |

[a] 6-311++G(d,p) basis set. [b] As cited in ref 47. [c] Values in parentheses represent the standard deviation.[26] [d] Reference 33.

**TABLE 2: Wavelengths (nm) Corresponding to the Computed Vertical Excitation Energies Compared with the Experimental Absorption Maxima (nm) for the Monomers of Formic Acid, Acetic Acid, and Benzoic Acid**

| excited state | major transition | TDDFT(LDA) | TDDFT(B3LYP) | CASSCF | MRCI | expt. | oscillator strength[k] |
|---|---|---|---|---|---|---|---|
| | | | Formic Acid | | | | |
| $S_1$ | 10a′−3a″ (n−$\pi$*) | 218 | 214 | 227 | 208 | 226-260,[a] 210−259.3,[b,c] 215[d] | 0.0010 |
| $S_2$ | 10a′−11a′ (n−$\sigma$*) | 184 | 172 | 181 | 164 | | 0.0347 |
| $S_3$ | 2a″−3a″ ($\pi$−$\pi$*) | 169 | 162 | 176 | 155 | 125-185,[c] 159[e] | 0.0414 |
| $T_1$ | 10a′−3a″ | 240 | 239 | 243 | 220 | | |
| $T_2$ | 2a″−3a″ | 203 | 214 | 211 | 185 | | |
| $T_3$ | 10a′−12a′ | 191 | 178 | 191 | 167 | | |
| | | | Acetic Acid | | | | |
| $S_1$ | 13a′−4a″ (n−$\pi$*) | 221 | 214 | 208 | 167 | 210,[c] 207,[f] 209[g] | 0.0006 |
| $S_2$ | 13a′−14a′ | 200 | 185 | 192 | 145 | | 0.0485 |
| $S_3$ | 2a″−3a″ ($\pi$−$\pi$*) | 182 | 170 | 169 | | 125−200,[c] 160[e] | 0.0009 |
| $T_1$ | 13a′−4a″ | 240 | 237 | 220 | 180 | | |
| $T_2$ | 3a″−4a″ | 204 | 209 | 196 | 159 | | |
| $T_3$ | 13a′−14a′ | 200 | 189 | 189 | 147 | | |
| | | | Benzoic Acid | | | | |
| $S_1$ | 27a′−6a″ (n−$\pi$*) | 291 | 273 | 190 | 221 | | 0.0 |
| $S_2$ | 5a″−6a″ ($\pi$−$\pi$*) | 270 | 255 | 181 | 205 | 280, 278,[i] 280[j] | 0.0206 |
| $S_3$ | 4a″−6a″ ($\pi$−$\pi$*) | 266 | 254 | 170 | | 230[h] | 0.1847 |
| $T_1$ | 4a′−6a″ | 320 | 352 | 220 | 261 | | |
| $T_2$ | 5a′−6a″ | 310 | 303 | 212 | 237 | | |

[a] Reference 10. [b] Reference 12. [c] Reference 11. [d] Reference 13. [e] Reference 16. [f] Reference 31. [g] Reference 32. [h] Reference 40. [i] Reference 42. [j] Reference 45. [k] DFT(B3LYP)/6-311++G(d,p).

1 and compared with the values reported from experimental studies. It is clear that the bond lengths and bond angles obtained from HF and DFT calculations are close to the experimental values. The HF calculation underestimates the bond lengths slightly, while the DFT/B3LYP calculation shows a maximum deviation of 0.003 Å only. The bond angles are overestimated by the HF method to a maximum of 3°, while the DFT results deviate from experimental results to a maximum extent of 1.6° only. Hence, the optimized geometries obtained from the DFT calculations were used to estimate the excitation energies by the TDDFT method.

For the CASSCF and MRCI computation of excitation energies, optimized geometries obtained from HF calculations were used. An active space of eight orbitals that included n, $\pi$, $\pi$*, and $\sigma$* orbitals with eight electrons was used. The wavelengths corresponding to the vertical excitation energies computed using the above methods are listed in Table 2.

Although it is not easy to identify uniquely the electronic transitions in terms of localized molecular orbitals such as n, $\pi$, $\pi$*, and $\sigma$*, we have tried to assign them on the basis of the major contributions, aided by schematic diagrams of the frontier orbitals. The first excited ($S_1$) state of FA arises from the 10a′−3a″ (n−$\pi$*) transition. TDDFT, CASSCF, and MRCI methods predict an excitation energy that agrees with the experimental result within the reported range of Ng and Bell.[12] They are also in close agreement with the experimental measurement of 215 nm by Singleton et al.[13] The $S_2$ state is due to the 10a′−11a′ (n−$\sigma$*) transition, and the excitation energy is predicted reasonably well by TDDFT(B3LYP) and MRCI methodologies. The third excited state could be from a 2a″−3a″ ($\pi$−$\pi$*) transition. The TDDFT result is very close to what was reported as the absorption maximum (159 nm) assigned to a $\pi$−$\pi$* transition by Nagakura et al.[16] It is worth mentioning here that our results are in better agreement with the experiment than those of Peyerimhoff and Buenker[50] and Demoulin.[51]

**3.2. Formic Acid Dimer.** The ground-state calculations for FAD were also carried out at HF/6-311++G(d,p) and DFT-(B3LYP,LDA)/6-311++G(d,p) levels of theory. The geometry of the dimer with the atom labels is shown in Figure 2. The dimerization energy for FAD was found to be 12.9 and 15.1 kcal/mol at HF and DFT (B3LYP) levels of theory, respectively. The dimerization energies after BSSE correction were found to be 12.2 and 14.7 kcal/mol, respectively, when compared to the experimental value of 14.8 kcal/mol.[17] The important geometrical parameters for the dimer are given in Table 3. The bond lengths calculated by the DFT (B3LYP) methodology are close to the experimental values, with a maximum deviation of 0.035 Å, and the bond angles deviate to a maximum of 3.6°. The HF calculations show much larger deviations than the DFT (B3LYP). A comparison of the experimental bond parameters for the monomer and the dimer reveals that the O−H and C═O bonds lengthen and the C−O bond shortens in going from the monomer to the dimer. Similar changes are predicted by both the HF and DFT (B3LYP) calculations. DFT (B3LYP) calculations suggest that the O−H and C═O bonds increase by 0.027 and 0.019 Å, respectively, while the C−O bond shortens by 0.033 Å. The HF calculations predict an increase of 0.012 and 0.014 Å in the bond lengths of O−H and C═O, respectively, and a decrease of 0.022 Å in the C−O bond length. The optimized geometries of the dimer in its ground electronic state as obtained from the different theoretical methods were used for the excited-state calculations in the respective methods.

**TABLE 3: Ground-State Geometric Parameters for the Dimers of Formic Acid, Acetic Acid, and Benzoic Acid**

| | FAD | | | AAD | | | BAD | | |
|---|---|---|---|---|---|---|---|---|---|
| param | HF[a] | DFT/B3LYP[a] | expt[b] | HF[a] | DFT/B3LYP[a] | expt[c] | HF[a] | DFT/B3LYP[a] | expt[d] |
| $r_{12}$(C−O)/Å | 1.299 | 1.313 | 1.320 | 1.307 | 1.323 | 1.334(0.004) | 1.306 | 1.322 | 1.275 |
| $r_{23}$(O−H)/Å | 0.959 | 0.998 | 1.033 | 0.959 | 0.998 | 1.03 | 0.960 | 0.999 | 1.000 |
| $r_{34}$(O···H)/Å | 1.865 | 1.701 | 1.720 | 1.842 | 1.683 | | 1.822 | 1.665 | |
| $r_{45}$(C═O)/Å | 1.191 | 1.218 | 1.217 | 1.197 | 1.226 | 1.231(0.003) | 1.200 | 1.230 | 1.263 |
| $\theta_{234}$/deg | 171.5 | 176.4 | 180.0 | 174.0 | 178.7 | | 179.5 | 179.6 | |

[a] 6-311++G (d,p) basis set. [b] As cited in ref 47. [c] Values in parentheses represent the standard deviation.[26] [d] As cited in ref 35.

**TABLE 4: Wavelengths (nm) Corresponding to the Computed Vertical Excitation Energies Compared with the Experimental Absorption Maxima (nm) for the Dimers of Formic Acid, Acetic Acid, and Benzoic Acid**

| excited state | major transition | TDDFT(LDA) | TDDFT(B3LYP) | CASSCF | MRCI | expt. | oscillator strength[g] |
|---|---|---|---|---|---|---|---|
| | | | Formic Acid Dimer | | | | |
| $S_1$ | $10b_u-3a_u$ | 232 | 210 | 174 | 171 | | 0.0 |
| $S_2$ | $10b_u-3b_g$ (n−$\pi$*) | 219 | 207 | 128 | 170 | 130−170,[a] 205[b] | 0.0028 |
| $S_3$ | $10a_g-3a_u$ | 214 | 179 | 134 | 129 | | 0.0006 |
| $T_1$ | $10b_u-3a_u$ | 243 | 230 | 184 | 182 | | |
| $T_2$ | $10b_u-3b_g$ | 227 | 227 | 184 | 181 | | |
| $T_3$ | $2a_u-3a_u$ | 222 | 216 | 176 | 131 | | |
| | | | Acetic Acid Dimer | | | | |
| $S_1$ | $13b_u-4a_u$ | 227 | 209 | 120 | 138 | | 0.0 |
| $S_2$ | $13a_g-4a_u$ (n−$\pi$*) | 226 | 206 | 117 | 134 | 164.8,[a] <205,[c] 203[d] | 0.0020 |
| $S_3$ | $13b_u-4b_g$ | 216 | 180 | 106 | | | 0.0006 |
| $T_1$ | $13b_u-4a_u$ | 235 | 227 | 163 | | | |
| $T_2$ | $13b_u-4b_g$ | 233 | 225 | 159 | | | |
| $T_3$ | $3a_u-4a_u$ | 218 | 210 | 117 | | | |
| | | | Benzoic Acid Dimer | | | | |
| $S_1$ | $27a_u-28a_u$ | 301 | 274 | | | | 0.0 |
| $S_2$ | $5b_g-28a_u$ ($\pi-\pi$*) | 300 | 274 | | | 280,[e] 285.2[f] | 0.0369 |
| $S_3$ | $26b_u-28a_u$ | 295 | 257 | | | | 0.0 |
| $S_4$ | $26b_u-6b_g$ | 294 | 251 | | | | 0.0002 |
| $T_1$ | $4b_g-28a_u$ | 322 | 353 | | | | |
| $T_2$ | $5a_u-28a_u$ | 320 | 353 | | | | |
| $T_3$ | $27a_u-28a_u$ | 317 | 306 | | | | |
| $T_4$ | $5b_g-28a_u$ | 316 | 306 | | | | |

[a] Reference 11. [b] Reference 13. [c] Reference 31. [d] Reference 32. [e] Reference 42. [f] Reference 41. [g] DFT(B3LYP)/6-311++G(d,p).

The excited-state energies were determined using the TDDFT method with both B3LYP and LDA functionals. For the CASSCF method, as in the case of the monomer, (8,8) active space that allows different excitations within the eight orbitals (four from each monomer) was used. The active orbitals were n, $\pi$, $\pi$*, and $\sigma$* in nature. The vertical excitation energies computed using the different methods are listed in Table 4.

The first excited singlet ($S_1$) state of FAD arises from an n−$\pi$* transition. It can be seen that the CASSCF and MRCI vertical excitation energies for the $S_0-S_1$ transition are close to the experimental values reported by Barnes and Simpson.[11] However, the TDDFT result is closer to the experimental value of Singleton et al.[13] To the best of our knowledge, there has not been any other theoretical study of the excited states of FAD.

The frontier orbitals (HOMO-1, HOMO, LUMO, and LUMO+1) of the monomer and the dimer of formic acid are shown in Figure 3. The correlation diagram of the four highest occupied MOs of the monomer and the dimer calculated at the B3LYP/6-311++G(d,p) level is given in Figure 4. The interaction between the two monomer units causes splitting of the different MOs. The nonbonding and the bonding $\sigma$ orbitals show larger splitting than the $\pi$ orbitals. The large splitting of the $\sigma$ orbitals is presumably due to the hydrogen bond being formed in plane with the $\sigma$ orbital orientations. The stabilizing effect of the nonbonding orbitals is expected to affect the excitation energies. The vertical excitation energy computed for the n−$\pi$* transition, for example, by TDDFT/B3LYP calculation, increases slightly in going from the monomer to the dimer, resulting in a slight blue shift (214 nm for FA and 210 nm for FAD), in accord with the experimental observation.

**3.3. Acetic Acid Monomer.** The various important geometrical parameters of acetic acid monomer as obtained from theory and experiment are included in Table 1. The bond distances calculated at both DFT (B3LYP) and HF levels of theory are very close to the experimental values. The ground-state geometries were used to compute the vertical excitation energies using TDDFT, CASSCF, and MRCI methodologies. For the CASSCF calculations seven active orbitals with six electrons distributed among them were used. The vertical excitation energies for the different low-lying excited states are given in Table 2.

The excitation energy for the first excitation state, arising from 13a′−4a″ (n−$\pi$*) transition is predicted well by TDDFT and CASSCF methods. As a matter of fact, the vertical excitation wavelength predicted by the CASSCF calculation is in quantitative agreement with the absorption maximum results reported by all the experimentalists. The deviation of the TDDFT (B3LYP) result is only by a few nm. Nagakura et al.[16] had observed an absorption peak at 160 nm and had identified it with $\pi-\pi$* transition. Here again, the TDDFT (B3LYP) result is close to the experimental finding.

**3.4. Acetic Acid Dimer.** The geometry of the cyclic dimer of acetic acid was optimized at DFT (B3LYP) and HF levels of theory with the same basis set as that used for formic acid, and the results agree very well with the available experimental results. Here again the DFT results are closer to experiment

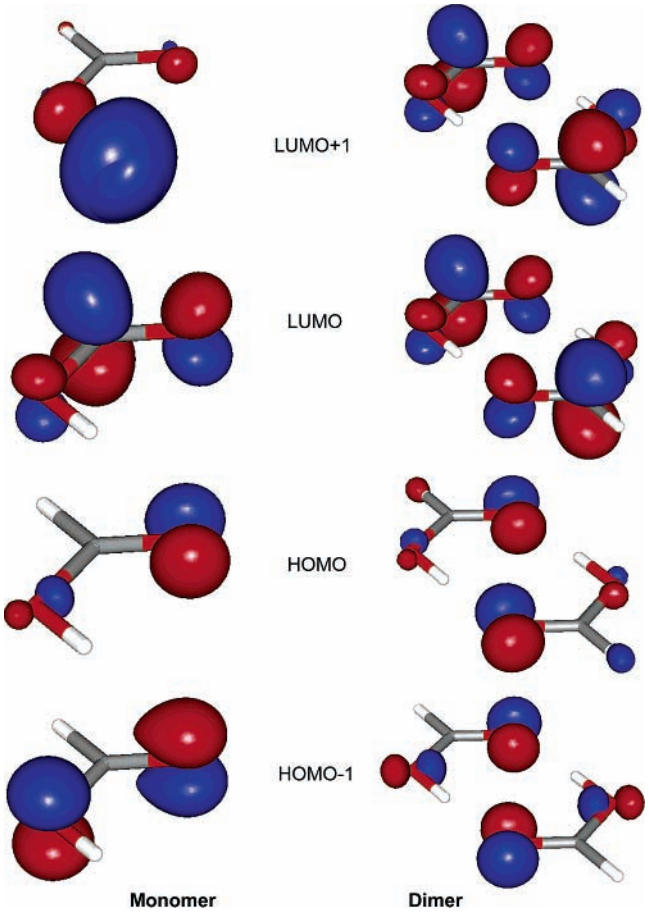


**Figure 3.** Frontier orbitals of the monomer and dimer of formic acid.

than HF. The dimerization energy for acetic acid was found to be 12.5 and 15.2 kcal/mol, respectively, by the HF and DFT-(B3LYP) calculations (including BSSE correction), when compared to the experimental value of 14.6 kcal/mol.[17]

For estimating the transition energies for the acetic acid dimer (AAD) using the CASSCF method, an active space of eight orbitals that included n, $\pi$, $\pi^*$, and $\sigma^*$ orbitals with eight electrons was used. The corresponding ground-state optimized geometries were used for the ab initio and TDDFT calculations. Table 4 shows the wavelengths corresponding to the vertical transition energies for acetic acid dimer for the first three singlet and triplet excited states. The experimental absorption spectrum of acetic acid dimer could not be resolved completely. Orlando and Tyndall[31] predicted the absorption maximum to occur at a wavelength shorter than 205 nm. Hintze et al.[32] recorded the absorption maximum at 203 nm. Theoretical results for the dimer obtained by the different methods are included in Table 4. The $S_1$ and $S_2$ states have a major contribution from n$-\pi^*$ transitions. It becomes clear that the TDDFT (B3LYP) predicts the excitation energy close to the experimental result, while the CASSCF and MRCI calculations tend to overestimate it. A larger active space might improve the CASSCF and MRCI excitation energies. As in the case of formic acid dimer, the excited states are found to be essentially due to the individual monomer excitations. Hence the $S_1$ and $S_2$ states are nearly degenerate as shown by the different methods. It is worth adding here that the TDDFT (B3LYP) calculations predict a slight blue shift in going from the monomer (214 nm) to the dimer (209 nm) in accord with the experiment. Barnes and Simpson[13] had observed the spectrum in the range of 130−180 nm and had interpreted it in terms of the n$-\pi^*$ or n$-\sigma^*$ transition.

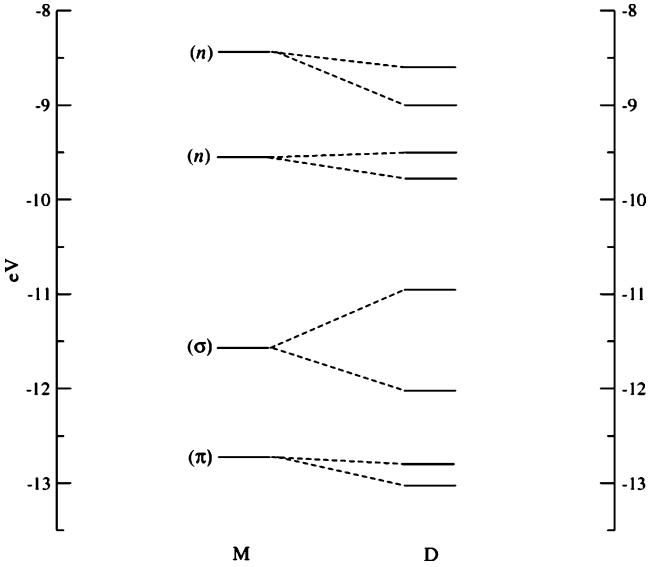


**Figure 4.** Correlation diagram between the four highest occupied molecular orbitals of the monomer (M) and the resulting molecular orbitals of the dimer (D) of formic acid.

Interestingly, the TDDFT (B3LYP) calculation predicts the third excited singlet state to occur at 180 nm.

**3.5. Benzoic Acid Monomer.** The ground-state geometry of benzoic acid monomer was optimized using HF and DFT methods. The resulting optimized geometry (see Table 1) was used for the excited-state calculations using TDDFT (LDA, B3LYP), CASSCF, and MRCI methodologies. An active space of seven orbitals with eight electrons was used for the CASSCF and MRCI calculations. The active space included n, $\pi$, and $\pi^*$ orbitals. The resulting wavelengths corresponding to the vertical excitation energies for the first three singlet and triplet states are listed in Table 2. The first excited singlet state arises from an n$-\pi^*$ (27a′$-$6a″) transition, whereas the second and the third states are due to $\pi-\pi^*$ (5a″$-$6a″ and 4a″$-$6a″) transitions. Three peaks (280, 230, and 190 nm) have been observed experimentally. The TDDFT calculations predict the wavelengths in the range of 254−270 nm. Both the CASSCF and MRCI calculations predict energy differences much larger than what is observed experimentally.

**3.6. Benzoic Acid Dimer.** Some of the geometrical parameters as obtained from HF and DFT calculations for the benzoic acid dimer (BAD) listed in Table 3 compare very well with the available experimental results. The dimerization energy (including BSSE correction) for benzoic acid was calculated at HF and DFT(B3LYP) levels of theory as 13.1 and 15.7 kcal/mol, respectively. The experimental stabilization energy for the dimer was reported to be 16.2 kcal/mol.[34]

The excited states for the benzoic acid dimer were treated only at the TDDFT (LDA and B3LYP) level of theory. Both CASSCF and MRCI calculations could not be carried out with the available computational resources. The TDDFT results are listed in Table 4 and compared with the available experimental value.[42] The first two excited states of the dimer result from transitions that are $\pi-\pi^*$ in nature. By symmetry, the $S_1$ state is not observable. TDDFT results are reasonably close to the experimental result for the $S_2$ state. TDDFT (LDA) calculations predict a slightly longer wavelength while the TDDFT (B3LYP) calculations predict a shorter wavelength, when compared to the experimental result. The first two excited states appear as doublets that are nearly degenerate, emphasizing that the monomer units in the dimer are hardly affected by the hydrogen bonds. A closer look (not shown) at the MOs gives an insight

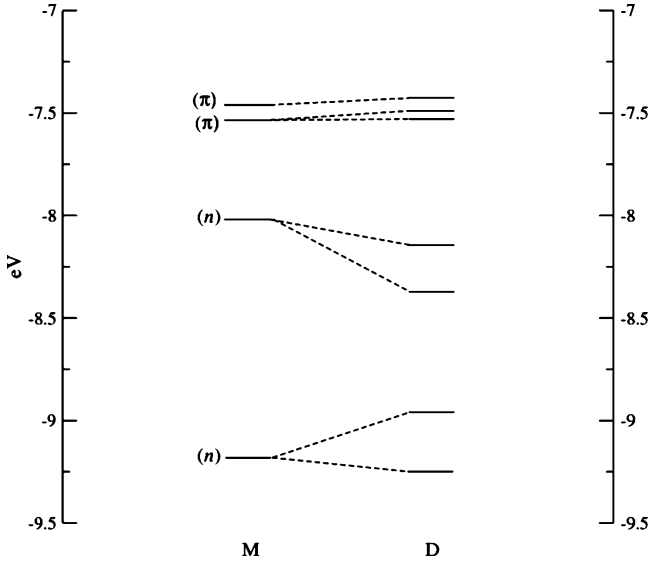


**Figure 5.** Correlation diagram for the highest occupied molecular orbitals of the monomer (M) and the resulting MOs of the dimer (D) of benzoic acid.

**TABLE 5: Ground-State Binding Energies of Carboxylic Acid Dimers**

| | binding energy/(kcal/mol) | | | |
|---|---|---|---|---|
| | HF[a] | DFT/B3LYP | | |
| dimers | | ZPE uncorrected[a] | ZPE corrected | expt |
| FAD | 12.9 (12.2) | 15.1 (14.7) | 13.3 | 14.8[b] |
| AAD | 13.3 (12.5) | 15.7 (15.2) | 14.3 | 14.6[b] |
| BAD | 13.9 (13.1) | 16.1 (15.7) | 14.9 | 16.2[c] |

[a] Values in parentheses are BSSE corrected. [b] Reference 17. [c] Reference 34.

into the (non)interaction. The correlation between the highest four occupied MOs of each monomer and the resulting eight MOs of the dimer is shown in Figure 5. The interaction between the ($\pi$) HOMOs of the monomers is negligible, and this results in nearly degenerate HOMOs in the dimer. A similar trend is observed for the interaction between the lower energy MOs, which are also $\pi$ orbitals. Interestingly, the nonbonding orbitals of the monomers interact with each other much more and are stabilized; they show a splitting of ~0.2 eV. Similar to the singlet states, the triplet states also appear as doublets for the dimers, as listed in Table 4, as they also arise from $\pi-\pi^*$ transitions.

The computed binding energies for the dimers listed in Table 5 show that they do not change much as one goes from FAD to BAD (changes are ≤1 kcal/mol), indicating that the effect of the methyl and phenyl groups on dimerization is negligible. The BSSE corrections for the dimers are also found to be <1 kcal/mol. Zero-point energy corrected binding energies were also estimated and are included in Table 5. They are comparable to the available experimental results. The ground-state optimized geometrical parameters obtained at the B3LYP/6-311++G (d,p) level, for both the monomer and the dimer of the three acids, are compared in Table 6. The C−O bond distance decreases (by ~0.03 Å) as one goes from the monomer to the dimer for each one of them. This suggests a decrease in the electron density in the C−O bond as the hydrogen bond is formed in the dimer. The expected decrease/increase in the bond lengths, due to hydrogen bond formation, is confirmed by natural bond orbital (NBO) analysis at the B3LYP/6-311++G (d,p) level of theory. The changes in the electron density in the lone pair (n) and antibonding ($\sigma^*$, $\pi^*$) orbitals on dimerization in FAD, AAD, and BAD are listed in Table 7. One of the lone pairs of O8 and the antibonding ($\sigma^*$) orbital of C1−O2 show a considerable decrease in the electron density that results in the strengthening of the C−O bond and hence the observed contraction of bond length. In NBO analysis, the interaction between the filled donor orbital ($i$) and the vacant acceptor ($j$) orbital can be approximated by the second-order perturbation expression

$$E(2) = -n_i \frac{\langle i|F|j\rangle^2}{\epsilon_j - \epsilon_i} = -n_i \frac{F_{ij}^{\ 2}}{\Delta E} \qquad (1)$$

where $\epsilon_i$ and $\epsilon_j$ are NBO energies, $n_i$ is the occupancy of the donor orbital, and ($F_{ij}$) is the Fock matrix element. Estimates of the second-order perturbative charge-transfer energies listed in Table 8 reveal large contributions arising from the interaction of the lone pairs of the carbonyl oxygen and O−H antibonding ($\sigma^*$) orbitals. The interaction between the second lone pair and the O−H ($\sigma^*$) orbital is larger than the one between the first lone pair and the O−H ($\sigma^*$). There is a small energy difference

**TABLE 7: Changes in the Electron Density in the Lone Pair (n) and Antibonding ($\sigma^*$, $\pi^*$) Orbitals on Dimerization for All Three Acids, from NBO Analysis[a]**

| NBO | FAD | AAD | BAD |
|---|---|---|---|
| *N*(O8) | −0.02035 | −0.01927 | −0.02170 |
| *N*(O8) | +0.00923 | +0.00362 | +0.00338 |
| $\sigma^*$(C1−O8) | +0.00503 | +0.00578 | +0.00580 |
| $\pi^*$(C1−O8) | +0.05318 | +0.05402 | +0.05679 |
| $\sigma^*$(C1−O2) | −0.02449 | −0.02675 | −0.02709 |
| $\sigma^*$(O2−H3) | +0.05081 | +0.05574 | +0.05857 |

[a] The atom labels are defined in Figure 2. Because of symmetry, results are shown only for one of the monomer units in the dimer.

**TABLE 6: Comparison of the Optimized Geometric Parameters for the Monomer and the Dimer of the Acids in the Ground Electronic State As Obtained from DFT/B3LYP/6-311++G(d,p) Calculation[a]**

| | FA | | AA | | BA | |
|---|---|---|---|---|---|---|
| param | monomer | dimer | monomer | dimer | monomer | dimer |
| C−O/Å | 1.346 | 1.313 | 1.358 | 1.323 | 1.359 | 1.322 |
| O−H/Å | 0.971 | 0.998 | 0.969 | 0.998 | 0.968 | 0.999 |
| O···H/Å | | 1.701 | | 1.683 | | 1.660 |
| C═O/Å | 1.199 | 1.218 | 1.205 | 1.226 | 1.209 | 1.230 |
| O···O/Å | | 2.698 | | 2.681 | | 2.664 |
| O−H···O/deg | | 176.4 | | 178.7 | | 175.3 |
| H···C═O/deg | | 126.8 | | 127.2 | | 126.8 |
| $\nu_{O-H}$/cm$^{-1}$ | 3585 | 3130 | 3609 | 3107 | 3621 | 3073 |
| | | 3037 | | 3014 | | 2984 |
| $\nu_{C=O}$/cm$^{-1}$ | 1742 | 1702 | 1744 | 1690 | 1714 | 1662 |
| | | 1638 | | 1642 | | 1618 |

[a] The vibrational frequencies are scaled by a factor of 0.96.

**TABLE 8: Second-Order Perturbation Analysis of the Interaction between Electron Donor and Acceptor Orbitals in NBO Basis[a]**

| donor NBO (*i*) | acceptor NBO (*j*) | $E(2)^b$/ (kcal/mol) | $\epsilon_j - \epsilon_i{}^c$/au | $F_{i,j}{}^d$/au |
|---|---|---|---|---|
| Formic Acid Dimer | | | | |
| from unit 1 to unit 2 | | | | |
| LP(1) O8 | BD*(1) O6−H7 | 8.44 | 1.09 | 0.086 |
| LP(2) O8 | BD*(1) O6−H7 | 17.42 | 0.69 | 0.100 |
| from unit 2 to unit 1 | | | | |
| LP(1) O4 | BD*(1) O2−H3 | 8.44 | 1.09 | 0.086 |
| LP(2) O4 | BD*(1) O2−H3 | 17.42 | 0.69 | 0.100 |
| Acetic Acid Dimer | | | | |
| from unit 1 to unit 2 | | | | |
| LP(1) O8 | BD*(1) O6−H7 | 7.95 | 1.08 | 0.083 |
| LP(2) O8 | BD*(1) O6−H7 | 20.08 | 0.71 | 0.108 |
| from unit 2 to unit 1 | | | | |
| LP(1) O4 | BD*(1) O2−H3 | 7.95 | 1.08 | 0.083 |
| LP(2) O4 | BD*(1) O2−H3 | 20.08 | 0.71 | 0.108 |
| Benzoic Acid Dimer | | | | |
| from unit 1 to unit 2 | | | | |
| LP(1) O8 | BD*(1) O6−H7 | 8.72 | 1.08 | 0.087 |
| LP(2) O8 | BD*(1) O6−H7 | 21.08 | 0.70 | 0.111 |
| from unit 2 to unit 1 | | | | |
| LP(1) O4 | BD*(1) O2−H3 | 8.72 | 1.08 | 0.087 |
| LP(2) O4 | BD*(1) O2−H3 | 21.10 | 0.70 | 0.111 |

[a] The atom labels are defined in Figure 2. [b] Hyperconjugative interaction energy. [c] Energy difference between donor (*i*) and acceptor (*j*) NBOs. [d] Fock matrix element between (*i*) and (*j*) NBOs.

between the electron donor and the acceptor NBOs, and in addition the Fock matrix element ($F_{ij}$) is large.

The observed increase in the O−H and C═O bond lengths, ∼0.03 and 0.02 Å, respectively, in going from the monomer to the dimer is also explained by NBO analysis. An examination of the changes in the electron density values reveals a large increase in the contribution of the antibonding $\sigma^*$ (O−H) and $\pi^*$ (C═O) orbitals, which weakens the bonds and results in their elongation. As discussed above, the carbonyl oxygens are the dominant electron donors, and the weakening of these bonds can be ascertained from the calculated vibrational stretch frequencies. The O−H and C═O vibrational stretching frequencies undergo a red shift upon dimerization.

The vertical excitation energies for the first excited state of the monomers of the three different carboxylic acids, estimated using different methods, are compared with the experimental results in Figure 6a. Both the TDDFT (B3LYP and LDA) results follow the experimental values closely with similar trends. The CASSCF values are close to the experimental excitation energies for formic acid and acetic acid but deviate significantly from the observed value for benzoic acid. MRCI results also show large deviations from the experimental transition energies for acetic acid and benzoic acid. The deviations of the CASSCF and MRCI excitation energies from the experimental values are likely due to the small active space chosen.

Vertical excitation energies of the first excited state of the dimers (Figure 6b) follow similar trends as for the monomers. The excitation energies of the formic acid and acetic acid dimers estimated by the TDDFT (B3LYP), CASSCF, and MRCI methodologies are blue-shifted when compared to that of the monomers, in agreement with the experimental observation.[13,32] For benzoic acid monomer, the first excited-state arises from an n−$\pi^*$ transition, which is not observed experimentally. The second excited-state arises from a $\pi-\pi^*$ transition and has been reported experimentally. The TDDFT (B3LYP) calculation shows the absorption wavelength for the $\pi-\pi^*$ transition in benzoic acid dimer to be red-shifted by ∼19 nm, in qualitative agreement with the experimental result that shows a slight red shift of 2−5 nm. The observed trends in the shift in the vertical excitation energies can be thought to arise from the difference in the hydrogen bonding energy for the various dimers, in the excited state, as illustrated in Figure 7. The dimerization energy was found to be 12.7 kcal/mol for both FAD and AAD in the excited state, for the ground-state geometry. However, when going from the monomer of BA to the dimer, the nature of the excitation involved for the first excited state changes from n−$\pi^*$ to $\pi-\pi^*$. The stabilization energy of the dimer for the $\pi-\pi^*$ excited state was calculated to be 16.8 kcal/mol. It should also be noted that the hydrogen bond formed in the dimers of formic acid and acetic acid stabilize the nonbonding orbitals (n) that are involved in the transition and hence there is a slight increase in the observed excitation energies as shown in Figure 5. However, in benzoic acid, the $\pi$ orbitals that are involved in the transitions are destabilized, resulting in a red shift in the absorption maximum.

The simulated absorption spectra for the (n−$\pi^*$) transition for the monomer and dimer of formic acid and acetic acid and the ($\pi-\pi^*$) transition for the monomer and dimer of benzoic acid are plotted in Figure 8. The absorption profiles were

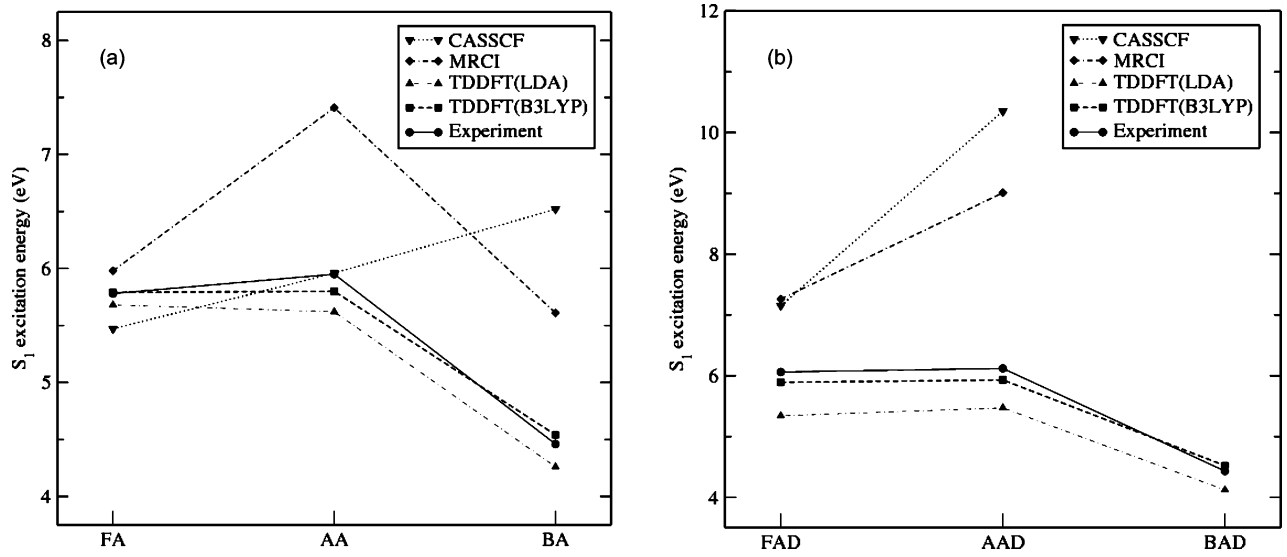


**Figure 6.** Vertical excitation energies (eV) for the $S_1$ state for the (a) monomers and (b) dimers of formic acid, acetic acid, and benzoic acid.

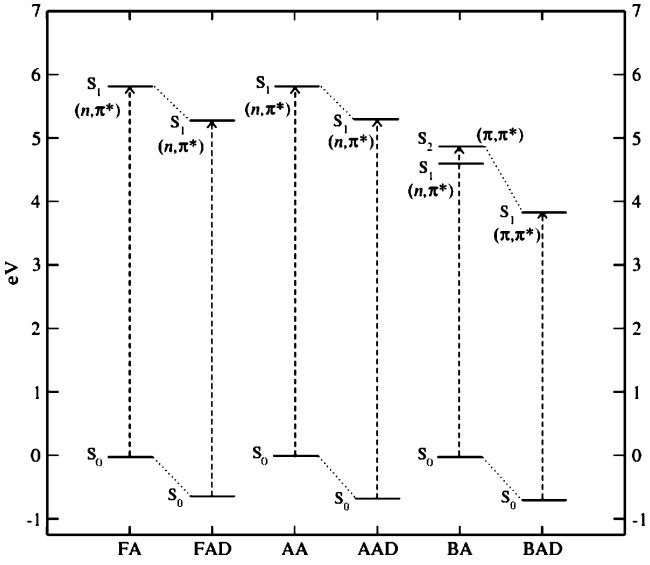


**Figure 7.** Correlation diagram for the ground and first excited states of the monomer and dimer of formic acid, acetic acid, and benzoic acid.

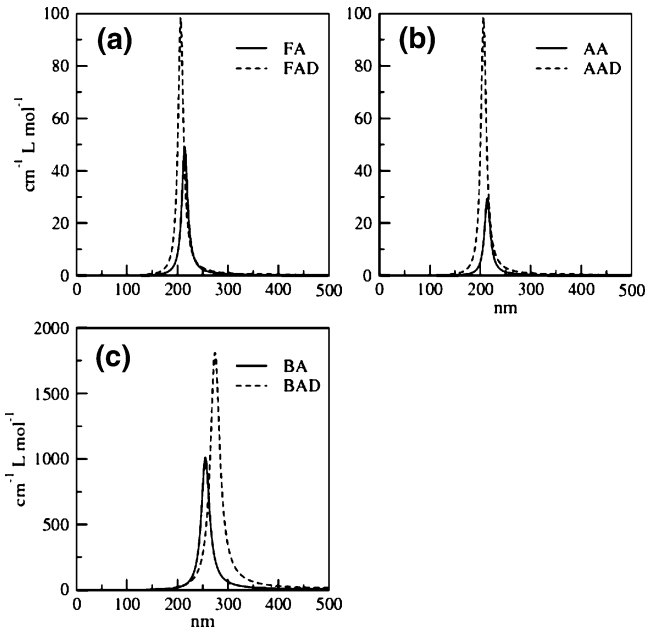


**Figure 8.** Simulated absorption spectrum of the monomer and dimer of (a) formic acid (n$-\pi^*$), (b) acetic acid (n$-\pi^*$), and (c) benzoic acid ($\pi-\pi^*$).

obtained using a Lorentzian model[63] given by

$$\epsilon(\omega) = a\sum_I \frac{f_I}{\Delta_{1/2,I}} \frac{0.25{\Delta_{1/2,I}}^2}{(\omega-\omega_I)^2 + 0.25{\Delta_{1/2,I}}^2} \qquad (2)$$

where $\epsilon$ is the molar absorbance in mol$^{-1}$ L cm$^{-1}$, $\Delta_{1/2,I}$ is the half-bandwidth, and $f_I$ is the oscillator strength. A half-bandwidth of 3000 cm$^{-1}$ was assumed, and the total integrated intensity was evaluated from the expression

$$4.319 \times 10^{-9} \int \epsilon(\omega)\, \mathrm{d}\omega = \sum_I f_I \qquad (3)$$

The simulated spectra show low intensities for the monomers and the dimers of formic acid and acetic acid, as they are of n$-\pi^*$ transitions with low oscillator strengths. The $\pi-\pi^*$ transitions in the case of benzoic acid monomer and dimer, on the other hand, have larger oscillator strengths and hence larger absorbance, as can be seen in Figure 8c. It is worth pointing out that, for each carboxylic acid, the intensity for the dimer is nearly double that for the monomer, in agreement with the experimental observation for acetic acid.

## 4. Summary and Conclusion

Geometries for the monomer and the dimer and the dimerization energies calculated for formic acid, acetic acid, and benzoic acid in their ground electronic states by DFT/B3LYP-(6-311++G(d,p)) are in excellent agreement with the available experimental results. Vertical excitation energies for the lowest energy electronic excitation in the monomer and the dimer of all three acids, computed using TDDFT (B3LYP) are also in very good agreement with the experimental results. The influence of the hydrogen bonds on the transition energies for the dimers is only marginal. The interaction between the two monomers seems to affect only the $\sigma$ bonds to some extent, as they are oriented in the molecular plane. Dimerization results in a slight blue shift (4−5 nm) in excitation energies for the first excited state of formic acid and acetic acid, due to the hydrogen bond formation, whereas in benzoic acid the hydrogen bonds formed destabilize the $\pi$ orbitals involved in the ($\pi-\pi^*$) transition, resulting in a red shift (∼19 nm) in accord with the experimental observations.

**Acknowledgment.** This study was supported in part by a grant from the Council of Scientific and Industrial Research, New Delhi. We are grateful to Drs. M. K. Harbola, T. Chakraborty, and S. Manogaran for valuable discussions.

## References and Notes

(1) Bellet, J.; Deldalle, A.; Samson, C.; Steenbeckeliers, G.; Wertheimer, R. *J. Mol. Struct.* **1971**, *9*, 65.
(2) Hocking, W. H. *Z. Naturforsch. A* **1976**, *31*, 1113.
(3) Bjarnov, E.; Hocking, W. H. *Z. Naturforsch., A* **1978**, *33*, 610.
(4) Willemot, E.; Dangoisse, D.; Monnanteuil, N.; Bellet, J. *J. Phys. Chem. Ref. Data* **1980**, *9*, 59.
(5) Vander Auwera, J. *J. Mol. Spectrosc.* **1992**, *155*, 136.
(6) Winnewisser, M.; Winnewisser, B. P.; Stein, M.; Birk, M.; Wagner, G.; Winnewisser, G.; Yamada, K. M. T.; Belov, S. P.; Baskakov, O. I. *J. Mol. Spectrosc.* **2002**, *216*, 259.
(7) Winnewisser, B. P.; Hocking, W. H. *J. Phys. Chem.* **1980**, *84*, 1771.
(8) Millikan, R. C.; Pitzer, K. S. *J. Chem. Phys.* **1959**, *27*, 1305.
(9) Miyazawa, T.; Pitzer, K. S. *J. Chem. Phys.* **1959**, *30*, 1076.
(10) Sugarman, B. *Proc. Phys. Soc.* **1943**, *55*, 429.
(11) Barnes, E. E.; Simpson, W. T. *J. Chem. Phys.* **1963**, *39*, 670.
(12) Ng. T. L.; Bell, S. *J. Mol. Spectrosc.* **1974**, *50*, 166.
(13) Singleton, D. L.; Paraskevopoulos, G.; Irwin, R. S. *J. Photochem.* **1987**, *37*, 209.
(14) Ioannoni, F.; Moule, D. C.; Clouthier, D. J. *J. Phys. Chem.* **1990**, *94*, 2290.
(15) Beaty-Travis, L. M.; Moule, D. C.; Lim, E. C.; Judge, R. H. *J. Chem. Phys.* **2002**, *117*, 4831.
(16) Nagakura, S.; Kaya, K.; Tsubomura, H. *J. Mol. Spectrosc.* **1964**, *13*, 1.
(17) Clague, A. D. H.; Bernstein, H. J. *Spectrochim. Acta A* **1969**, *25*, 593.
(18) Matylitsky, V. V.; Riehn, C.; Gelin, M. F.; Brutschy, B. *J. Chem. Phys.* **2003**, *119*, 10553.
(19) Halupka, M.; Sander, W. *Spectrochim. Acta A* **1998**, *54*, 495.
(20) Ito, F.; Nakanaga, T. *Chem. Phys.* **2002**, *277*, 163.
(21) Georges, R.; Freytes, M.; Hurtmans, D.; Kleiner, I.; Vander Auwera, J.; Herman, M. *Chem. Phys.* **2004**, *305*, 187.
(22) Madeja, F.; Havenith, M. *J. Chem. Phys.* **2002**, *117*, 7162.
(23) Smedarchina, Z.; Fernandez-Ramos, A.; Siebrand, W. *Chem. Phys. Lett.* **2004**, *395*, 339.
(24) Smedarchina, Z.; Fernandez-Ramos, A.; Siebrand, W. *J. Chem. Phys.* **2005**, *122*, 134309.
(25) Carnovale, F.; Livett, M. K.; Peel, J. B. *J. Chem. Phys.* **1979**, *71*, 255.
(26) Derissen, J. L. *J. Mol. Struct.* **1971**, *7*, 67.

(27) Vab Eijck, B. P.; Van Opheusden, J.; Van Schaik, M. M. M.; Van Zoerun, E. *J. Mol. Spectrosc*. **1991**, *86*, 865.
(28) Nguyen, M. T.; Sengupta, D.; Raspoet, G.; Vanquickenborne, L. G. *J. Phys. Chem.* **1995**, *99*, 11883.
(29) Ovaska, M. *J. Phys. Chem*. **1984**, *88*, 5981.
(30) Häber, T.; Schmitt, U.; Emmeluth, C.; Suhm, M. A. *Faraday Discuss*. **2001**, *118*, 331.
(31) Orlando, J. J.; Tyndall, G. S. *J. Photochem. Photobiol., A* **2003**, *157*, 161.
(32) Hintze, P. E.; Aloisio, S.; Vaida, V. *Chem. Phys. Lett*. **2001**, *343*, 159.
(33) Bruno, G.; Randaccio, L. *Acta Crystallogr*. **1980**, *B36*, 1711.
(34) Allen, G.; Wathinson, J. G.; Webb, K. H. *Spectrochim. Acta* **1966**, *22*, 807.
(35) Nagaoka, S.; Hirota, N.; Matsushita, T.; Nishimoto, K. *Chem. Phys. Lett*. **1982**, *92*, 498.
(36) Remmers, K.; Meerts, W. L.; Ozier, I. *J. Chem. Phys*. **2000**, *112*, 10890.
(37) Florio, G. M.; Sibert, E. L.; Zwier, T. S. *Faraday Discuss. Chem. Soc*. **2001**, *118*, 315.
(38) Bakker, J. M.; Aleese, L. M.; Helden, G. v.; Meijer, G. *J. Chem. Phys*. **2003**, *119*, 11180.
(39) Ito, M.; Tsukioka, H.; Imanishi, S. *J. Am. Chem. Soc*. **1960**, *82*, 1559.
(40) Baum, J. C.; McClure, D. S. *J. Am. Chem. Soc*. **1979**, *101*, 2335.
(41) Baum, J. C.; McClure, D. S. *J. Am. Chem. Soc*. **1980**, *102*, 720.
(42) Meijer, G.; de Vries, M. S.; Hunziker, H. E.; Wendt, H. R. *J. Phys. Chem*. **1990**, *94*, 4394.
(43) Poeltl, D. E.; McVey, J. K. *J. Chem. Phys.* **1983**, *78*, 4349.
(44) Poeltl, D. E.; McVey, J. K. *J. Chem. Phys*. **1984**, *80*, 1801.
(45) Nandi, C. K.; Chakraborty, T. *J. Chem. Phys*. **2004**, *120*, 8521.
(46) Brinkmann, N. R.; Tschumper, G. S.; Yan, G.; Schaefer, H. F. *J. Phys. Chem. A* **2003**, *107*, 10208.
(47) Jursic, B. S. *J. Mol. Struct. (THEOCHEM)* **1997**, *417*, 89.
(48) Chang, Y.; Yamaguchi, Y.; Miller, W. H.; Schaefer, H. F. *J. Am. Chem. Soc.* **1987**, 7245.
(49) Gora, R. W.; Grabowski, S. J.; Leszczynski, J. *J. Phys. Chem. A* **2005**, *109*, 6397.
(50) Peyerimhoff, S. D.; Buenker, R. J. *J. Chem. Phys*. **1969**, *50*, 1846.
(51) Demoulin, D. *Chem. Phys*. **1976**, *17*, 471.
(52) Parr, R. G.; Yang, W. *Density Functional Theory of Atoms and Molecules*; Oxford University Press: Oxford, U.K., 1989.
(53) Bauernschmitt, R.; Ahlrichs, R. *Chem. Phys. Lett*. **1991**, *256*, 454.
(54) Stratmann, R. E.; Scuseria, G.; Frisch, M. J. *J. Chem. Phys*. **1998**, *109*, 8218.
(55) Lee, C.; Yang, W.; Parr, R. G. *Phys. Rev. B* **1988**, *37*, 785.
(56) Becke, A. D. *J. Chem. Phys*. **1993**, *98*, 5648.
(57) Werner, H.-J.; Knowles, P. J. *J. Chem. Phys*. **1985**, *82*, 5053.
(58) Knowles, P. J.; Werner, H.-J. *Chem. Phys. Lett*. **1985**, *115*, 259.
(59) Werner, H.-J.; Knowles, P. J. *J. Chem. Phys*. **1988**, *89*, 5803.
(60) Knowles, P. J.; Werner, H.-J. *Chem. Phys. Lett*. **1988**, *145*, 514.
(61) Frisch, M. J.; Trucks, G. W.; Schlegel, H. B.; Scuseria, G. E.; Robb, M. A.; Cheeseman, J. R.; Zakrzewski, V. G.; Montgomery, J. A., Jr.; Stratmann, R. E.; Burant, J. C.; Dapprich, S.; Millam, J. M.; Daniels, A. D.; Kudin, K. N.; Strain, M. C.; Farkas, O.; Tomasi, J.; Barone, V.; Cossi, M.; Cammi, R.; Mennucci, B.; Pomelli, C.; Adamo, C.; Clifford, S.; Ochterski, J.; Petersson, G. A.; Ayala, P. Y.; Cui, Q.; Morokuma, K.; Salvador, P.; Dannenberg, J. J.; Malick, D. K.; Rabuck, A. D.; Raghavachari, K.; Foresman, J. B.; Cioslowski, J.; Ortiz, J. V.; Baboul, A. G.; Stefanov, B. B.; Liu, G.; Liashenko, A.; Piskorz, P.; Komaromi, I.; Gomperts, R.; Martin, R. L.; Fox, D. J.; Keith, T.; Al-Laham, M. A.; Peng, C. Y.; Nanayakkara, A.; Challacombe, M.; Gill, P. M. W.; Johnson, B.; Chen, W.; Wong, M. W.; Andres, J. L.; Gonzalez, C.; Head-Gordon, M.; Replogle, E. S.; Pople, J. A. *Gaussian 98*, revision A.11.1; Gaussian, Inc.: Pittsburgh, PA, 2001.
(62) MOLPRO is a package of ab initio programs written by Werner, H.-J.; and Knowles, P. J. with contributions from Amos, R. D.; Bernhardsson, A.; Berning, A.; Celani, P.; Cooper, D. L.; Deegan, M. J. O.; Dobbyn, A. J.; Eckert, F.; Hampel, C.; Hetzer, G.; Korona, T.; Lindh, R.; Lloyd, A. W.; McNicholas, S. J.; Manby, F. R.; Meyer, W.; Mura, M. E.; Nicklass, A.; Palmieri, P.; Pitzer, R.; Rauhut, G.; Schütz, M.; Stoll, H.; Stone, A. J.; Tarroni, R.; Thorsteinsson, T.
(63) Gorelsky, S. I. SWizard program, revision 3.6; http://www.sg-chem.net/.